

Understanding Space Radiation in Earth Environment with Radiation Data Portal

Viacheslav Sadykov¹, Zachary Watkins¹, William Jones¹, Dustin Kempton¹, Xiaochun He¹, Ashwin Ashok¹, W Kent Tobiska², Christopher Mertens³, Shubha Ranjan⁴, Irina Kitiashvili⁴, Ryan Spaulding⁴, Donald Dearthoff⁴
¹Georgia State University, ²Space Environment Technologies, ³NASA Langley Research Center, ⁴NASA Ames Research Center

Introduction to Radiation Data Portal

The impact of radiation dramatically increases at high altitudes in the Earth's atmosphere and in space. Therefore, monitoring and access to radiation environment measurements are critical for estimating the radiation exposure risks of aircraft and spacecraft crews and the impact of space weather disturbances on electronics. Addressing these needs requires reliable access to multi-source radiation environment data and enhanced visualization and search capabilities. The Radiation Data Portal provides an interactive web-based application for convenient search and visualization of in-flight radiation measurements.



Access the Radiation Data Portal at <https://data.nasa.gov/helio/portals/rdp/> or use a QR-code above

Radiation Portal Data Sources:

- The Automated Radiation Measurements for Aerospace Safety (ARMAS) data, augmented with the integrated flight parameters and environment. The ARMAS project utilizes a micro-dosimeter integrated into a data processing and communication package to measure and report the absorbed dose rates at a 1 min cadence.
- GOES Soft X-ray (SXR) radiation in the 0.5-4 Å and 1-8 Å channels. The Radiation Portal currently uses calibrated 1-min averaged soft X-ray fluxes measured by Geostationary Operational Environmental Satellite (GOES). Each measurement during the flight is connected to the nearest-time SXR measurement.
- Integrated GOES proton flux measurements. The Portal utilizes 5-min integrated calibrated measurements of the proton fluxes above the 1 MeV - 100 MeV. Each measurement during the flight is connected to the closest-in-time GOES measurement.

Radiation Data Portal Features:

- The back-end MySQL relational database is optimized for fast data retrieval.
- The Application Programming Interface (API) and Python routines have been developed to retrieve the database records directly, without interaction with the web interface.
- The application search engine contains a variety of filters (flight location and timing, environmental and dosimetric properties) allowing a user to customize flight selection.
- The search process and flight summary are supported by dynamic histograms of the flight parameters implemented with the Google Charts API and OpenLayers map API.

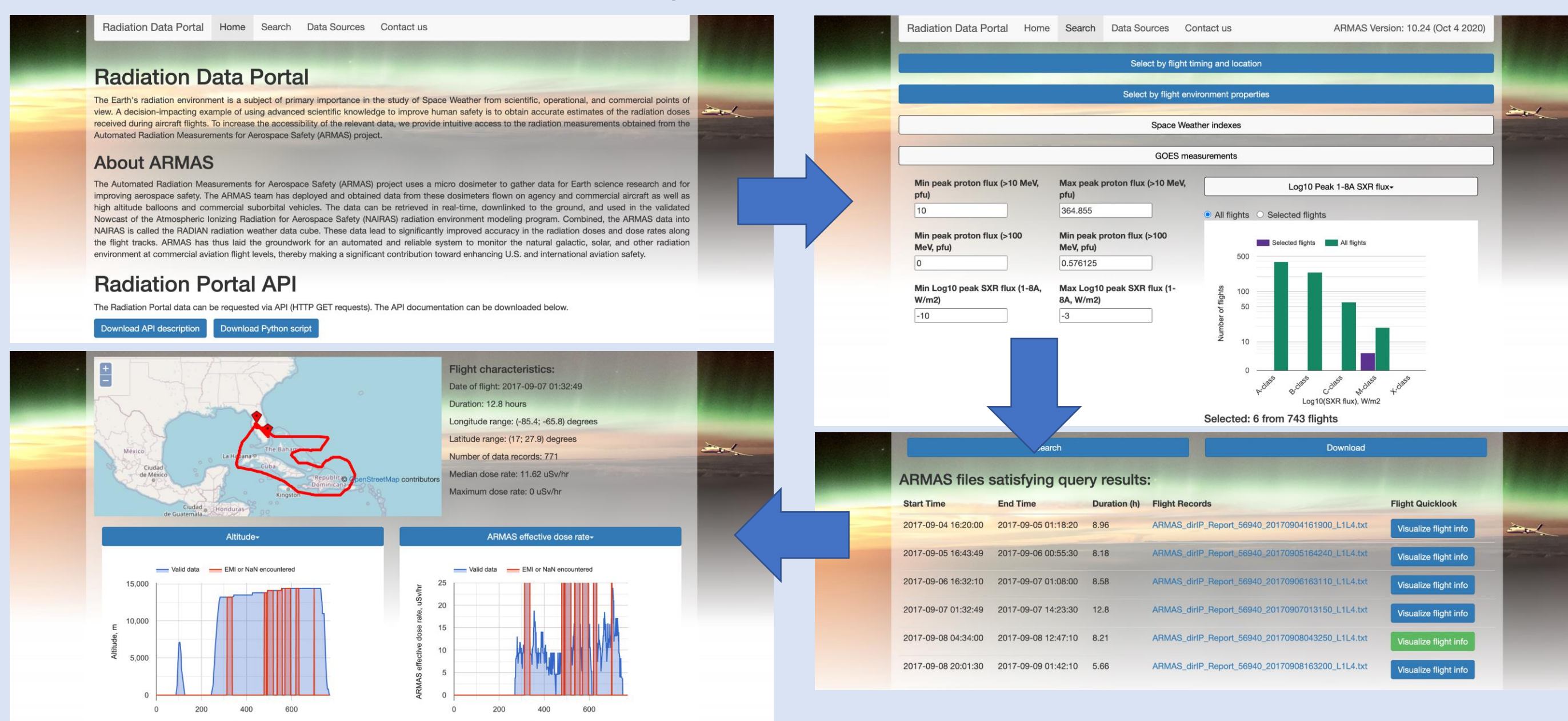


Figure 1. Illustration of the Radiation Data Portal web application, from the portal home page to the flight query result.

Expansion of Radiation Data Portal

Within the NASA HITS 2022 program grant, we are expanding the portal. Our specific goals are:

- Inclusion of additional radiation measurement sources (NASA ACE & DSCOVR, NASA CDAWeb geomagnetic activity data, ground-based neutron monitor measurements, measurements of cosmic ray muons, etc.). See Figure 2 for the entity relationship diagram.
- Expansion of ARMAS flight data catalog and enhancement of NAIIRAS dose rate modeling by using run-on-request flight trajectory tool
- Adaptation of the existing data visualization capabilities to the new data sets and improving the search engine
- Creation of the ML-ready data set for in-flight radiation prediction.

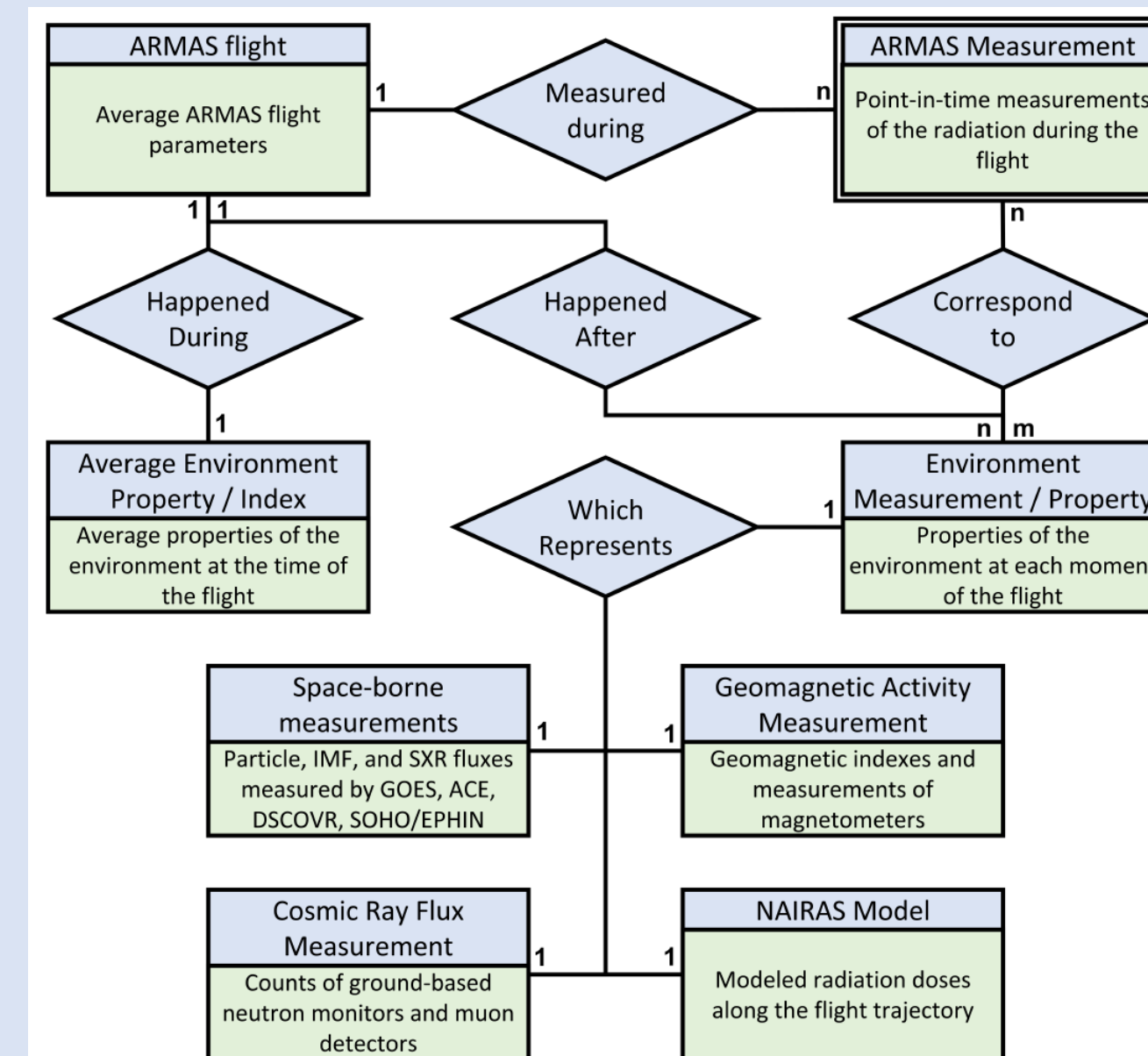


Figure 2. The entity relationship diagram of the enhanced Radiation Data Portal

We envision that the Radiation Data Portal will enhance our knowledge about solar-terrestrial interactions and Space Weather and that it will grow into a comprehensive collaborative effort involving many sides of our community.

Analysis of Radiation Measurements in Earth Atmosphere

ARMAS Measurements During Solar Proton Events

- Six ARMAS flights occurred during Solar Proton events (SP-enhanced conditions; an increase of the >10 MeV proton flux above the 10 pfu level).
- All SP-enhanced flights were performed in September 2017 in a confined geographic region. We collected the flights that happened in the same region during September 2016 – September 2018 when no SP events were observed (SP-low group).
- The Student's and Welch's t-tests demonstrate that there is no statistically-significant difference between the ARMAS/NAIRAS* ratios and median effective dose rates for SP-enhanced and SP-low groups of flights (see Figure 3 for distributions). *NAIRAS: Nowcast of Aerospace Ionizing Radiation System.
- Possible explanation is that most of energetic protons were in the low-energy tail and did not penetrate deep into the atmosphere

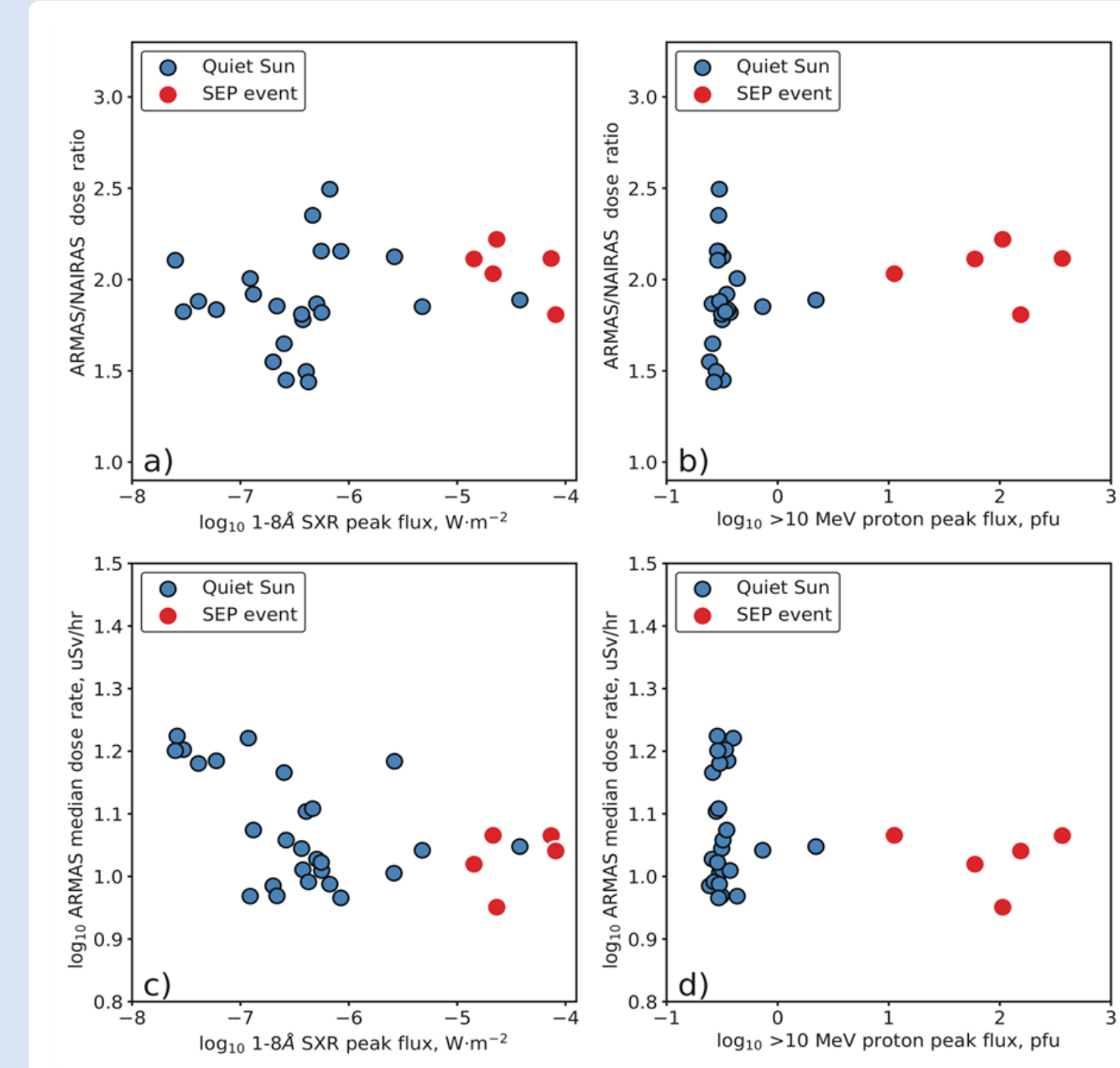


Figure 3. Correlations between the total dose ratios of ARMAS to NAIIRAS to X-ray flux (panel a) and proton flux above 10 MeV (b). Dependence of the ARMAS median effective dose rate from the X-ray flux (panel c) and proton flux above 10 MeV (d).

Statistical Analysis of ARMAS measurements

- Our goal is to perform a statistical analysis of the measured ARMAS dose rates and compare them with the predictions of the NAIIRAS v2 model at different locations (geomagnetic latitudes and altitudes) and states of solar and geomagnetic activity (geomagnetic indexes and the progression of the solar cycle)
- Our preliminary results indicate that the disagreements between the NAIIRAS v2 model and ARMAS data increase at lower geomagnetic latitudes (Figure 6) and vary with the solar cycle phase (Figure 8). The disagreement also typically increases with the height.

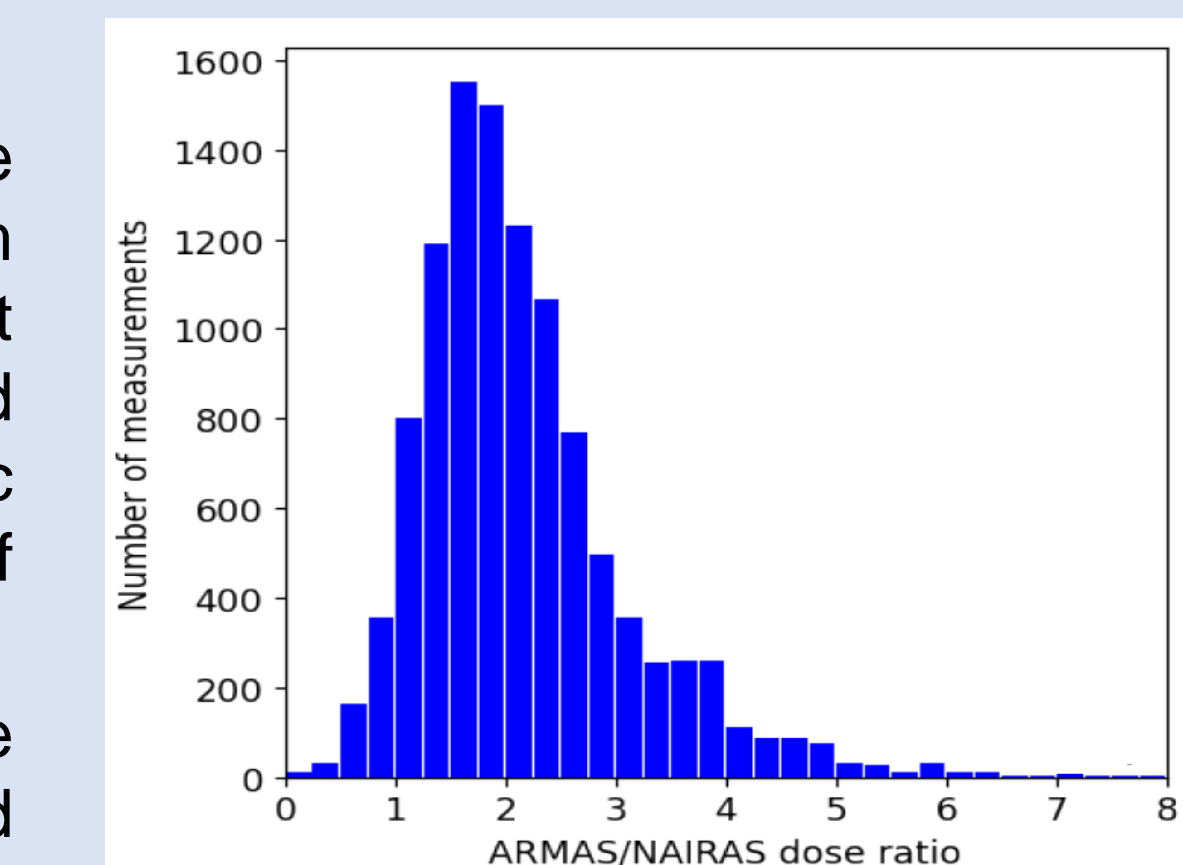


Figure 4. A histogram of ARMAS to NAIIRAS v2 dose ratios obtained for the confined space region: (-80 deg, -50 deg) lon, (5 deg, 35 deg) lat, (10 km, 15 km) alt

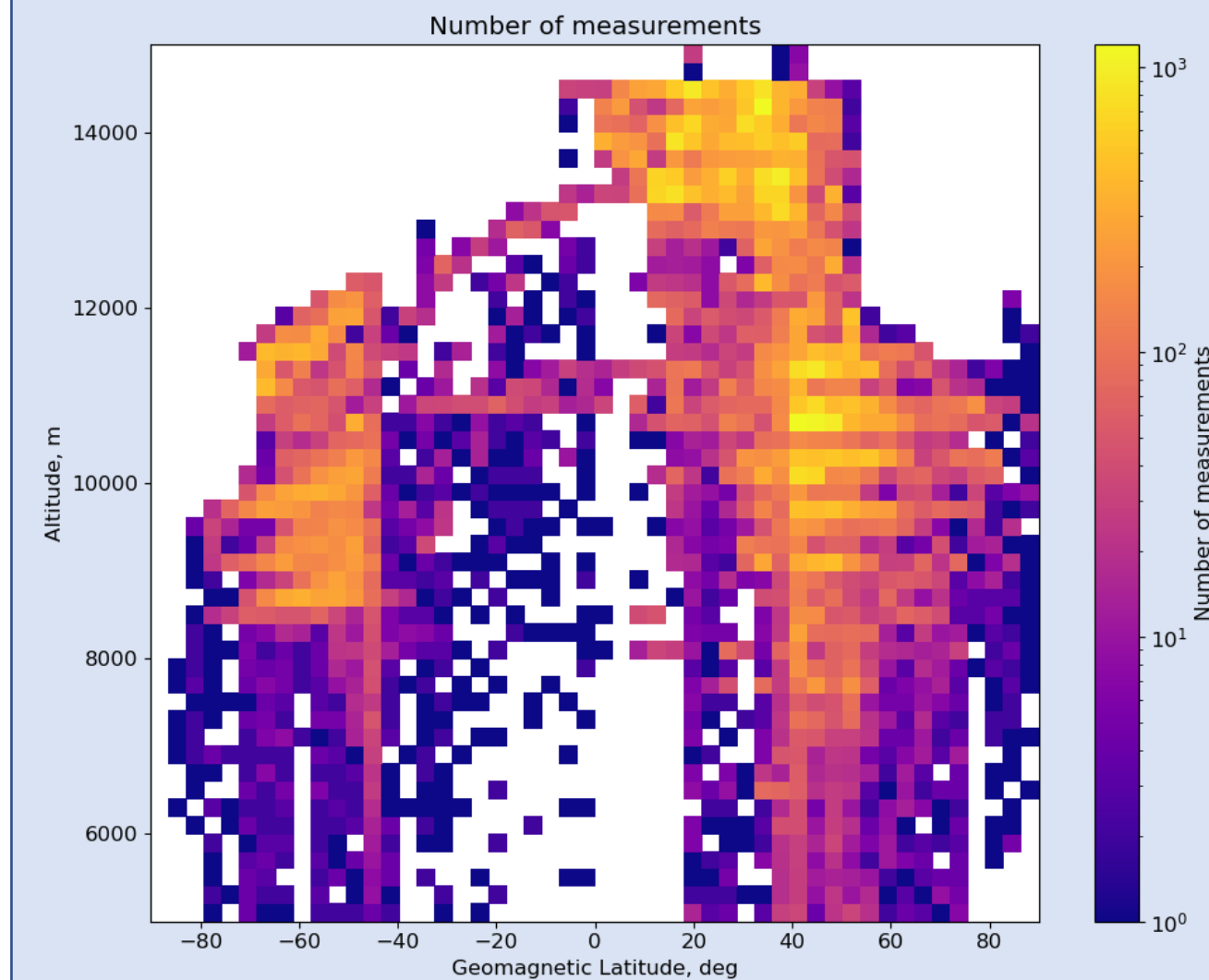


Figure 5. Coverage of geomagnetic latitude and altitude by ARMAS data (2013-2020).

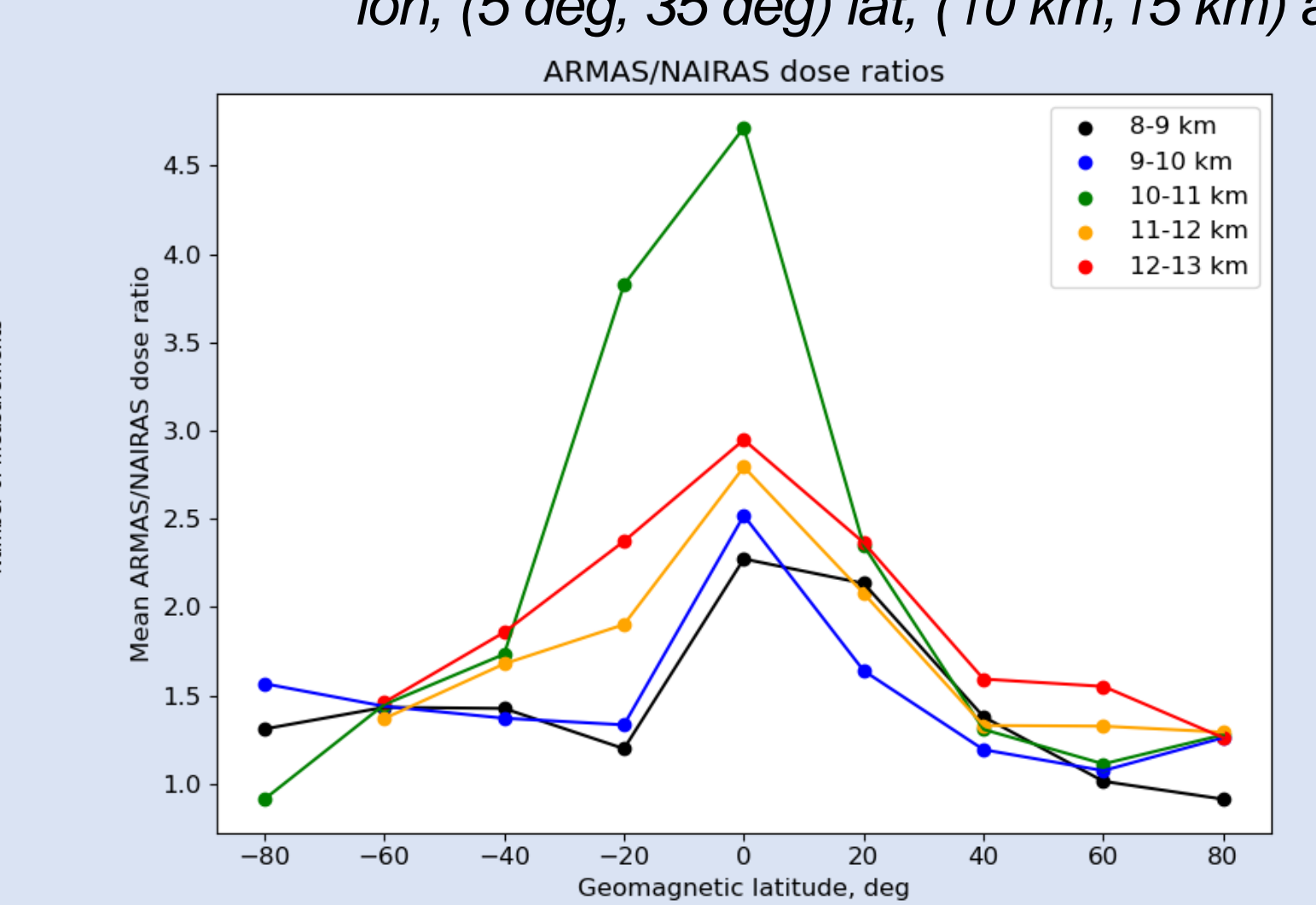


Figure 6. Mean ARMAS / NAIIRAS v1 dose ratios as functions of the geomagnetic latitude.

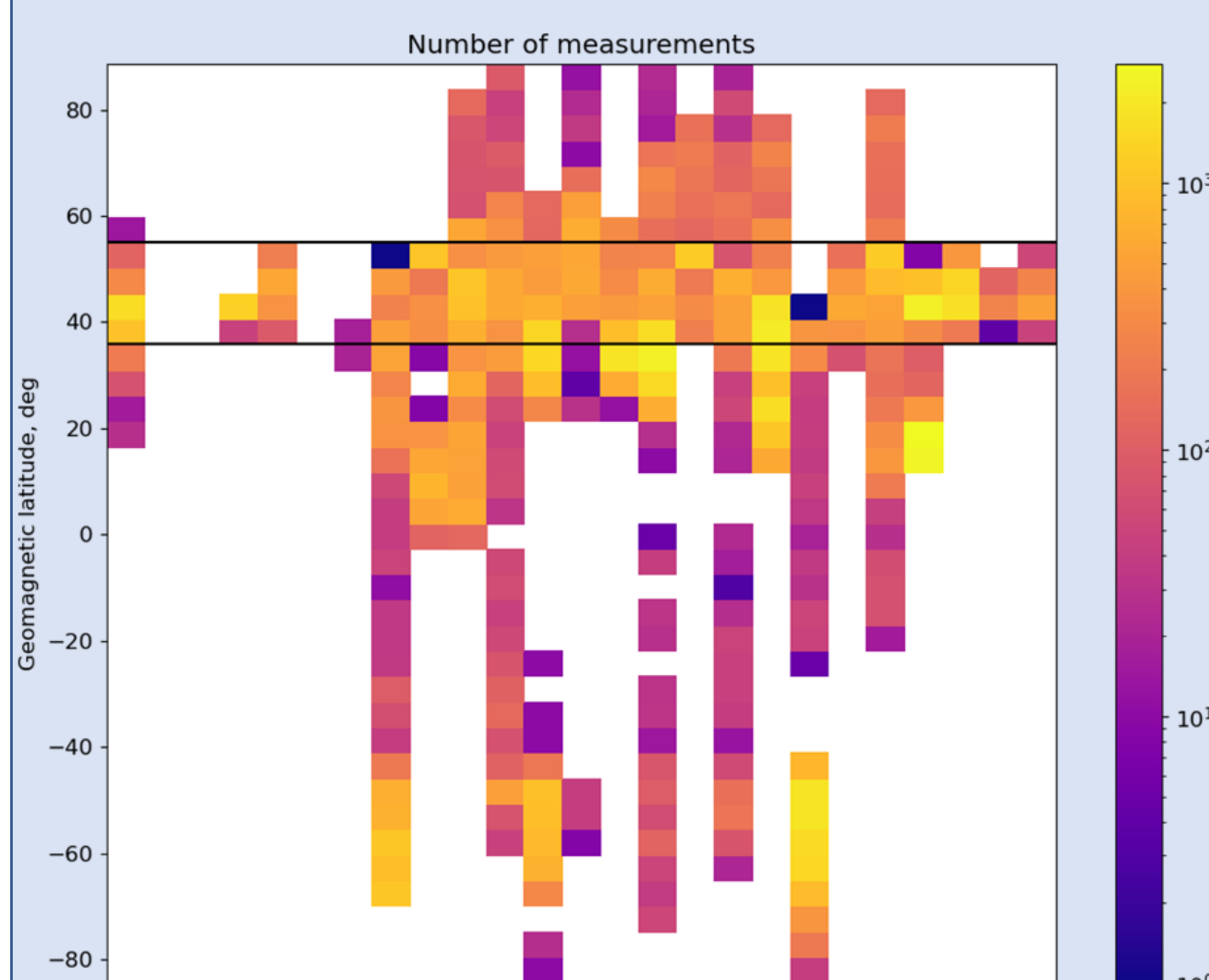


Figure 7. Selection of geomagnetic latitudes for a temporal variation analysis.

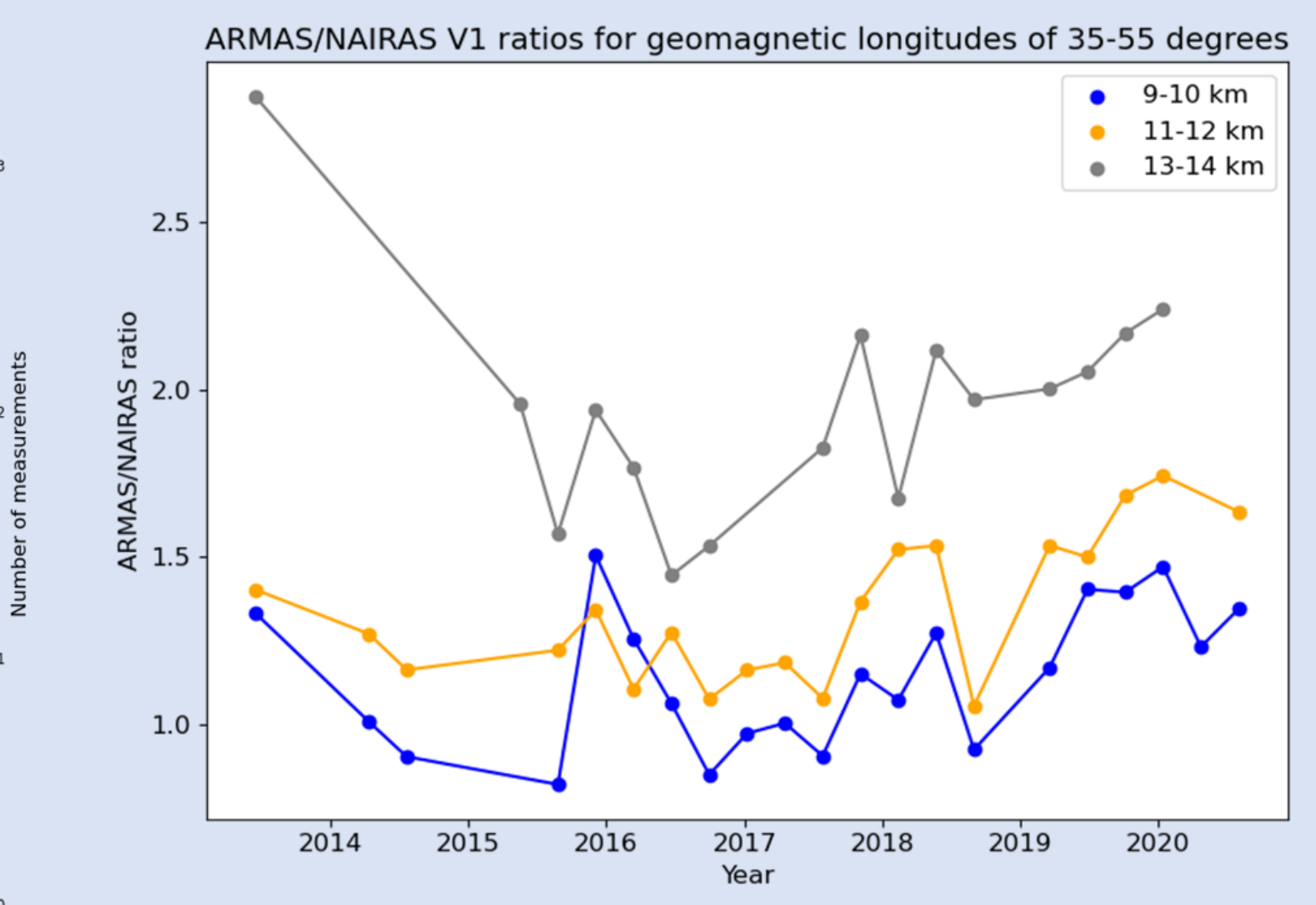


Figure 8. Mean ratios of the measured ARMAS radiation dose rates to the rates modeled by NAIIRAS v1 at geomagnetic latitudes of 35-55 degrees as functions of height and time.

Cosmic Ray Muon Measurements on an Airplane Flight

- We recorded cosmic ray muon flux using a cubeSat prototype detector (3 scintillator stack, scintillator size 9cm x 9cm x 1cm) onboard the Colombo (Sri Lanka) -> Doha (Qatar) -> Atlanta (USA) flight
- Our measurements indicate the variations of the muon particle counts with the flight altitude and route, and confirm the functionality of the developed cubeSat prototype
- Credits: Xiaochun He and Ashwin Ashok



Figure 9. Setup of the cubeSat prototype detector (top) and the illustrations of the flight route (bottom).

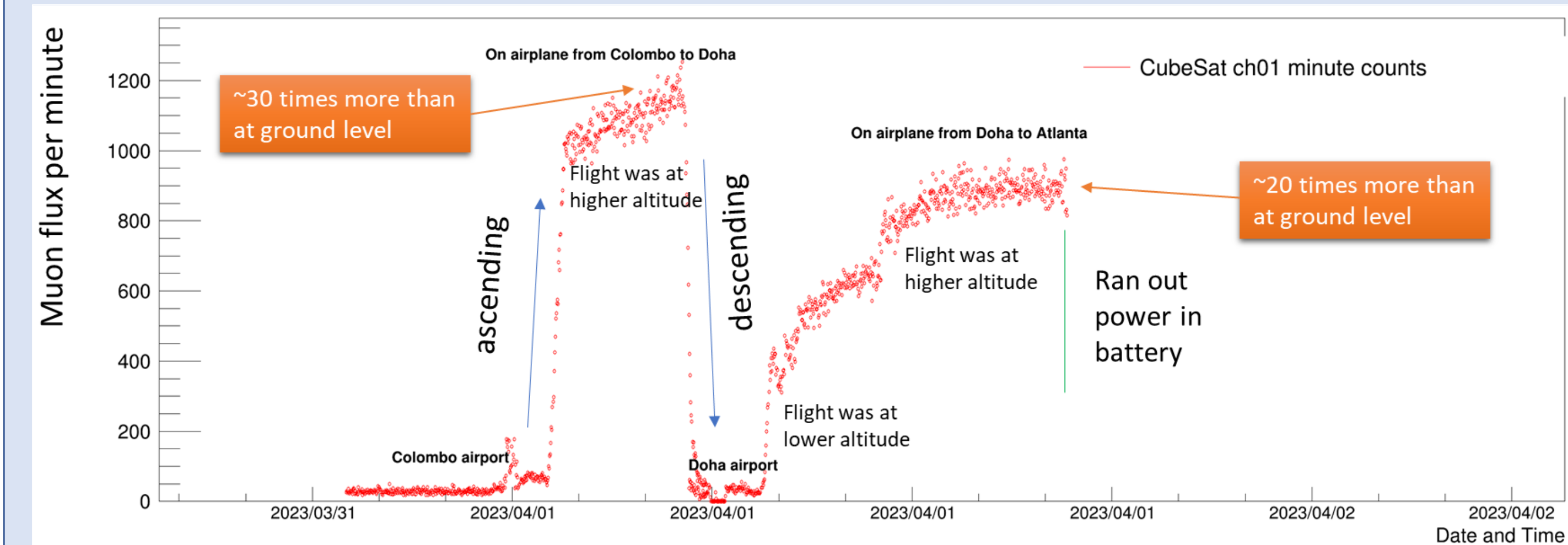


Figure 10. Measurements of the muon flux during the Colombo – Doha – Atlanta flight.

See poster by Arfa Mubashir (Poster #7, Thursday, April 20, and online) to find more results from the ground-based network of portable muon detectors developed in GSU and their sensitivity to space weather events

Prediction of Solar Energetic Particle Events

Solar Energetic Particle (SEP) are one of the major contributors to the radiation environment in Earth's upper atmosphere, magnetosphere, and space. Within the NASA ESI project "Machine Learning Tools for Predicting Solar Energetic Particle Hazards" we are enhancing the predictive capabilities of the SEPs by:

- Developing an online-accessible database that integrates the solar and heliospheric data, metadata, and descriptors related to SEPs
- See an online poster by Alexander Kosovichev "Development of Solar Energetic Particle Prediction Portal (SEP3)"
- Developing "all-clear" forecasts of SEPs with low false-alarm rates using a state-of-art machine learning approaches and several-cycle-long series of data
- See online posters by Aatiya Ali, Patrick O'Keefe, and Paul Kosovich

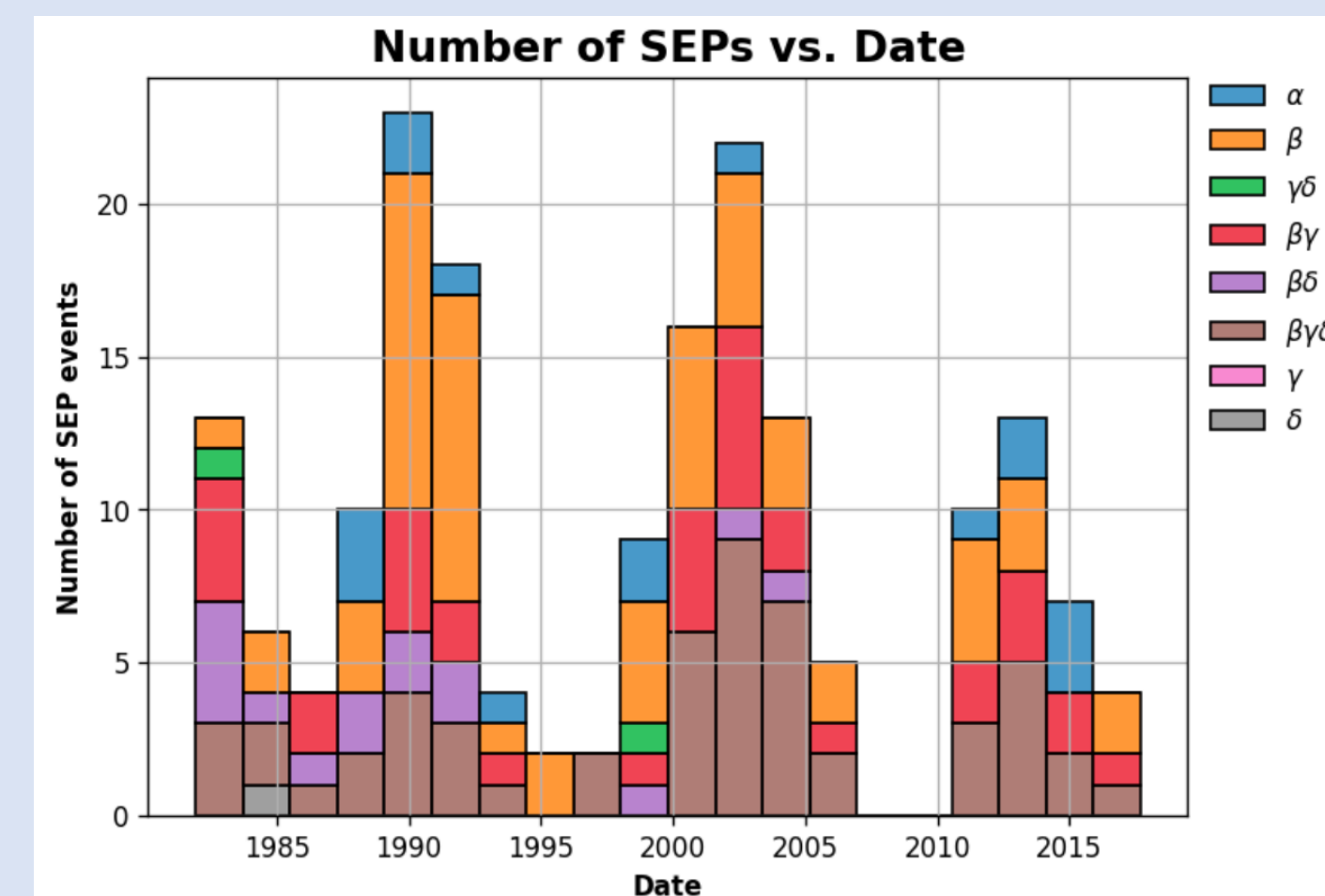
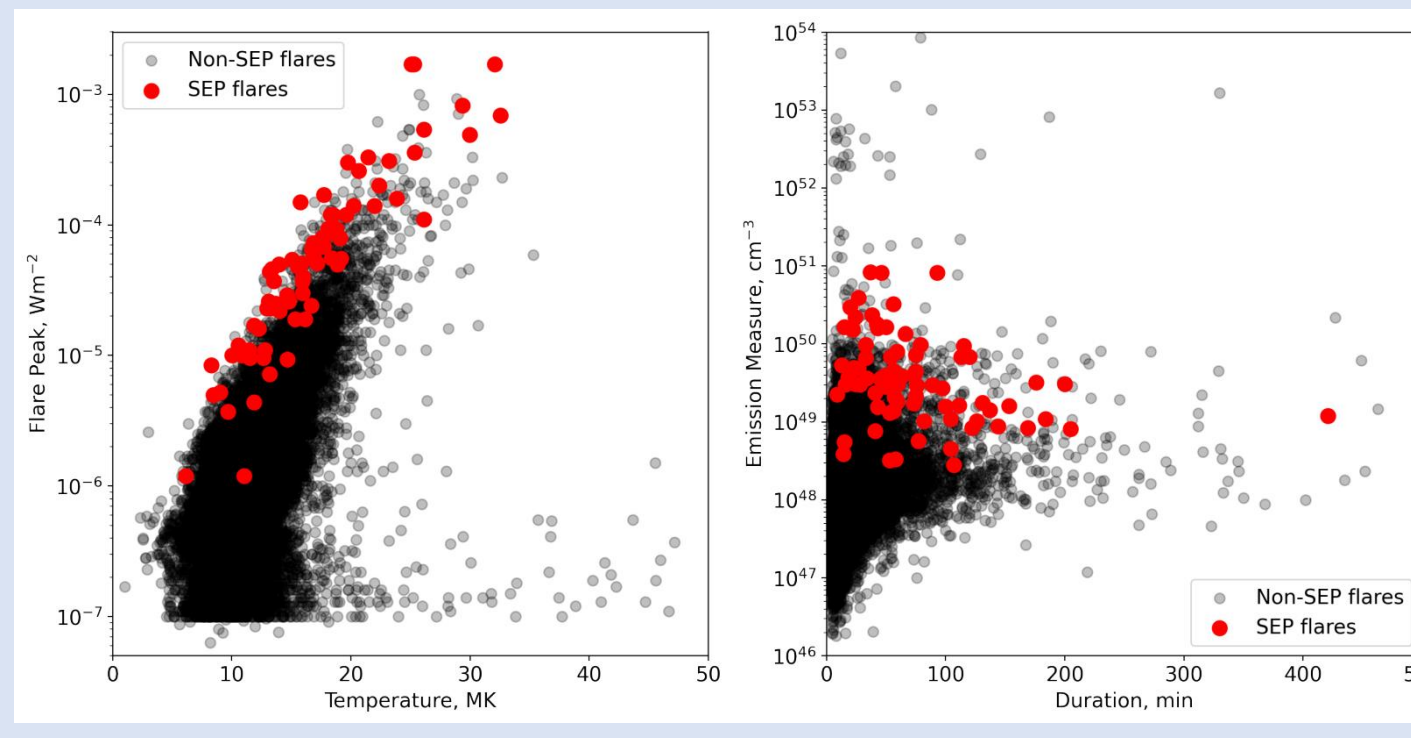


Figure 11. The number of SEP events produced from the active regions of different Hale classes as a function of time.

Figure 12. Flare peak emissions at 1-8Å and flare peak temperatures (left), and flare durations and peak emission measures (right)



Acknowledgements

We acknowledge NASA Ames Research Center for the use of computational resources and support of the Radiation Data Portal deployment. ARMAS data and corresponding NAIIRAS models were provided by Space Environment Technologies. We thank the GOES team for the availability of high-quality scientific data. The presented work was supported by the NASA HITS grant 80NSSC22K1561, GSU RISE Challenge grant, NASA ESI grant 80NSSC20K0302, and NSF FDSS grant 1936361.